IEEE Photonics Journal
An IEEE Photonics Society Publication

Open Access

Temperature and Crack Measurement Using Distributed Optic-Fiber Sensor Based on Raman Loop Configuration and Fiber Loss

Volume 11, Number 4, August 2019

Jian Li
Tao Yu
Mingjiang Zhang, *Member, IEEE*
Jianzhong Zhang
Lijun Qiao
Tao Wang

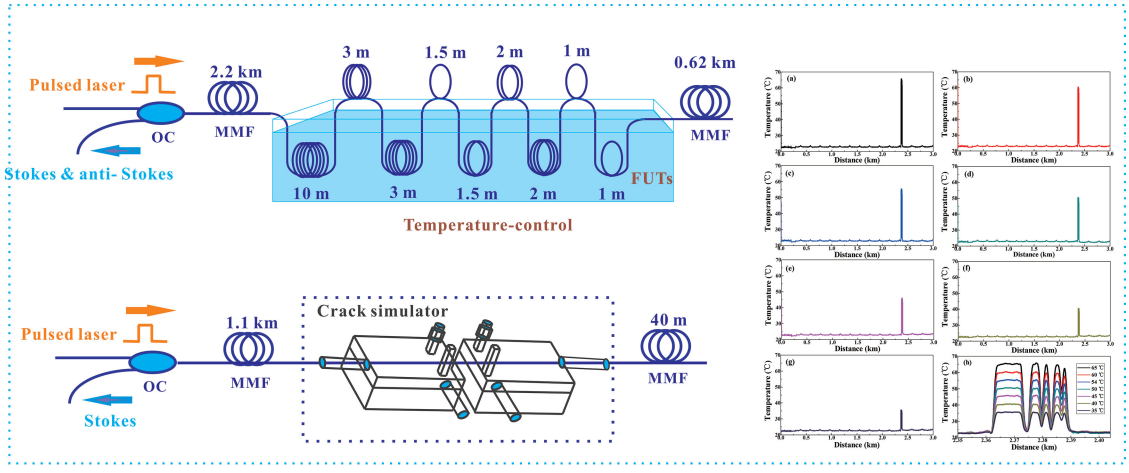

Distributed Optic-fiber Sensor

Temperature and Crack Measurement Using Distributed Optic-fiber Sensor Based on Raman Loop Configuration and Fiber Loss

DOI: 10.1109/JPHOT.2019.2931306

Temperature and Crack Measurement Using Distributed Optic-Fiber Sensor Based on Raman Loop Configuration and Fiber Loss

Jian Li,[1,2] Tao Yu,[1,2] Mingjiang Zhang ,[1,2] *Member, IEEE*, Jianzhong Zhang ,[1,2] Lijun Qiao,[1,2] and Tao Wang[1,2]

[1]College of Physics and Optoelectronics, Taiyuan University of Technology, Taiyuan 030024, China
[2]Key Laboratory of Advanced Transducers and Intelligent Control Systems (Ministry of Education and Shanxi Province), Taiyuan University of Technology, Taiyuan 030024, China

DOI:10.1109/JPHOT.2019.2931306

Manuscript received May 22, 2019; revised July 19, 2019; accepted July 23, 2019. Date of publication June 26, 2019; date of current version August 7, 2019. This work was supported in part by the National Natural Science Foundation of China under Grant 61527819 and Grant 61875146, in part by the Key R&D Program (high-tech field) of Shanxi Province (201803D121064), in part by the Research Project by Shanxi Province Youth Science and Technology Foundation under Grant 201601D021069, in part by the Research Project Supported by Shanxi Scholarship Council of China under Grant 2016-036 and Grant 2017-052, in part by the Program for the Outstanding Innovative Teams of Higher Learning Institutions of Shanxi, and in part by the Program for Sanjin Scholar. Corresponding author: Mingjiang Zhang (e-mail: zhangmingjiang@tyut.edu.cn).

Abstract: In recent years, optic-fiber sensors have been required to simultaneously measure the structure's crack and environmental temperature in the infrastructure monitoring system. We proposed and experimentally demonstrated a distributed optic-fiber sensor based on the Raman loop configuration and fiber loss characteristic for detecting the temperature and structure's crack. Among them, the Raman loop configuration with reference fiber is proposed to detect the temperature profile along the sensing fiber. It can eliminate the influence of external physical perturbation on the temperature measurement results, and do not require pre-calibration process before measurement. The temperature experimental results show that the temperature accuracy and spatial resolution can reach up to 0.28 °C and 1.2 m with the response time of 1.04 s. In addition, the information of crack is extracted by using the loss characteristics of Stokes, which is based on optical time domain reflectometry. The experiment results indicate that the fiber loss coefficient keeps a good linear variation between the crack ranges of 1.6 mm and 5.6 mm. The studies achieve the temperature and crack measurement only by one fiber.

Index Terms: Optic-fiber sensors, temperature and crack measurement, loop configuration, fiber loss.

1. Introduction

Distributed optic-fiber sensors exploit specific optical effects along the sensing fiber to obtain a spatially distributed physics profile [1]–[3]. It offers unique attributes and capabilities compared with the conventional discrete sensing methods. With its advantages of no-electromagnetic interference and long-sensing distance, the distributed fiber-optic sensors have become a research hotspot.

And the technology based on the fiber-optic sensors have been widely applied in the fields of gas pipeline, road tunnel and smart grids [4]–[6].

In recent years, the infrastructure monitoring systems such as road tunnels requires optic-fiber sensors to simultaneously measure temperature and structure's crack with high-speed [7]–[9]. At present, the methods for crack and temperature measurement using fiber-optic sensors mainly include Raman fiber-sensors [10]–[12], Fiber Bragg Grating (FBG) sensors [13]–[15] and Brillouin fiber-sensors [16]–[19]. Among them, the Raman fiber-sensors are only used for temperature detection for its temperature sensitive effect [10]. The Raman fiber-sensors are only used for temperature detection because the Raman scattering is sensitive to temperature only. The FBG sensors are quasi-distributed sensors with high resolution and measurement accuracy [13]–[15]. But the FBG sensors are limited in the application of long-distance detection [20], [21], such as the long-distance tunnel group monitoring. The Brillouin fiber-sensors can extract the temperature or strain information (crack causes strain on the fiber) by using the Brillouin frequency shift, which mainly includes the time-domain demodulation systems (BOTDR, BOTDA) [16], [17] and correlation-domain demodulation systems (BOCDR BOCDA) [18], [19] according to the demodulation principle. The above Brillouin fiber-sensors are based on the linear relationship of Brillouin frequency shift [22], [23], which means that the temperature and crack information cannot be measured without the pre-calibration process.

To solve the above problems, the first method is to place a temperature-insensitive reference fiber for achieving temperature compensation, then attaining the crack information. Subsequently, the combined sensor with dual-scattering is proposed [24]–[26]. Among them, the dual-scattering combined sensor based on the Brillouin-scattering and Raman-scattering, which can use the Raman fiber-sensor to detect the temperature along the sensing fiber, and extract the crack information by using the Brillouin fiber-sensor. For example, Gabriele Bolognini *et al.* demonstrated a hybrid Raman and Brillouin sensor with enhanced performance thanks to the combined use of standard Fabry–Perot lasers in conjunction with optical pulse coding techniques [24]. It achieved a temperature/strain resolution of 0.27 K/30 $\mu\varepsilon$. Crucially, it can simultaneously measure the temperature and strain along the sensing fiber compared to the above technology. The combined optic-fiber sensors can realize the multi-parameter measurement along the sensing fiber. However, the devices of combined optic-fiber sensors for infrastructure monitoring are complex and expensive (including electro-optic modulator, signal generator, *et al.*), and the polarization state of sensing fiber and lower measurement speed also affects the performance of combined system.

In this paper, we propose and experimentally demonstrate a novel distributed optic-fiber sensor based on the Raman loop configuration and fiber loss characteristic for detecting the temperature and structure's crack. The Raman loop configuration with a reference fiber can detect the temperature along the sensing fiber, and the information of crack is extracted by using the loss characteristics of Stokes based on OTDR technology. In addition, the demodulation devices only include two photodetectors, amplifiers and a data acquisition card, which omits the expensive devices such as electro-optic modulators and signal generators. The experimental results show that the temperature accuracy and spatial resolution can reach up to 0.28 °C and 1.2 m under the response time of 1.04 s, respectively. The crack information can be extracted using fiber loss, and the loss coefficient keeps a good linear variation between the crack ranges of 1.6 mm and 5.6 mm. This paper provides a new idea for simultaneous temperature and crack measurement with high-speed by using optic-fiber sensors.

2. Principle

2.1 Loop Configuration With Reference Fiber for Temperature Measurement

In Raman distributed temperature sensors (R-DTS), the principle of Raman scattering is based on the energy exchange in the sensing fiber. When the incident light quantum and fiber material molecules cause an inelastic collision in the sensing fiber, the light quantum releases or absorbs phonons which produce a Stokes light with a central wavelength of 1663 nm and an anti-Stokes light

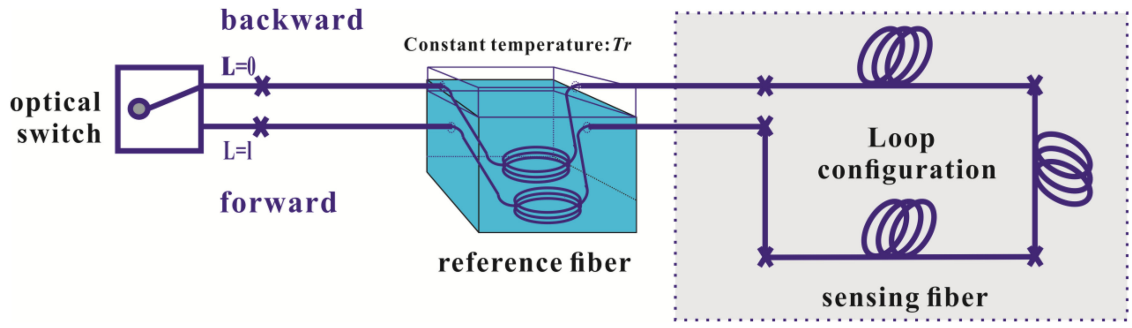

Fig. 1. Loop configuration with reference fiber.

with a central wavelength of 1450 nm. Among them, the anti-Stokes light is sensitive to temperature. The R-DTS can use it as a signal channel and the Stokes light as a reference channel [10], [11].

At present, there are two types of temperature demodulation systems in R-DTS, which include self-demodulation and dual-demodulation systems. The self-demodulation only uses the Raman anti-Stokes backscattered light to determine the temperature profile [12], [27], [28]. The self-demodulation system can optimize the temperature measurement accuracy due to the improvement of signal-to-noise ratio. It has achieved a temperature measurement accuracy of 1.58 °C over 11.5 km sensing distance [12]. The dual-demodulation system uses the ratio of anti-Stokes light over Rayleigh light [29] or Stokes light [10], [30]–[31]. Compared to the self-demodulation system, dual-demodulation system can optimize the temperature stability due to the calibration of Stokes signal. It has achieved a temperature stability of 0.7 °C over 10.22 km sensing distance [10]. However, the above systems cannot solve the problem for the temperature measurement error of R-DTS being induced by external physical perturbation. For solving this problem, the loop configuration of R-DTS with self-demodulation has been proposed. The loop configuration of RDTS sets the sensing fiber into a loop shape. Then the RDTS can obtain the forward and backward Raman backscattered signal. Marcelo A. Soto *et al.* use the R-DTS system based on loop configuration to demodulate the temperature information along the 19 km fiber [32]. Crucially, it can compensate for the external physical perturbation by obtaining the forward and backward Raman backscattered signal. But this method requires a traditional pre-calibration stage, that means the R-DTS system should place the entire fiber to a constant temperature condition before measurement. In measurement stage, if any device is replaced, it must be calibrated again.

In this letter, we add a section of reference fiber in the loop configuration, as shown in the Fig. 1. The function of reference fiber can avoid the pre-calibration stage before measurement. Among them, the fiber inside the dashed rectangle stands for the sensing fiber. The specific implementation process is as follows: the backward scattering intensity ratio of Stokes over the anti-Stokes signal can be expressed as:

$$\frac{\phi_{sb}}{\phi_{ab}} = \frac{K_s}{K_a}\left(\frac{\upsilon_s}{\upsilon_a}\right)^4 \exp\left(-\frac{h\Delta v}{kT}\right) \exp\left[(\alpha_a - \alpha_s)\, L\right]. \tag{1}$$

Where ϕ_{sb} and ϕ_{ab} are the backward scattering intensity of Stokes and anti-Stokes respectively, K_a and K_s are coefficients of anti-Stokes and Stokes scattering cross section, υ_a and υ_s are the optical frequencies of anti-Stokes and Stokes respectively, h is the Planck's constant, Δv is the Raman frequency shift of the fiber, k is the Boltzmann constant, T is the temperature, α_a and α_s are the attenuation coefficients of anti-Stokes and Stokes respectively, and L is the scattering position. After switching the light channel, the forward scattering intensity ratio of Stokes over the anti-Stokes signal can be obtained from Eq. (2).

$$\frac{\phi_{sf}}{\phi_{af}} = \frac{K_s}{K_a}\left(\frac{\upsilon_s}{\upsilon_a}\right)^4 \exp\left(-\frac{h\Delta v}{kT}\right) \exp\left[(\alpha_a - \alpha_s)\,(l - L)\right]. \tag{2}$$

Where ϕ_{sf} and ϕ_{af} are the forward scattering intensity of Stokes and anti-Stokes respectively, l stand for the length of sensing fiber. The Raman intensity in the loop configuration can be obtained from the geometric mean of backward (Eq. 1) and forward (Eq. 2) directions according to

$$\sqrt{\frac{\phi_{sb}}{\phi_{ab}}\frac{\phi_{sf}}{\phi_{af}}} = \frac{K_s}{K_a}\left(\frac{\upsilon_s}{\upsilon_a}\right)^4 \exp\left(-\frac{h\Delta v}{kT}\right)\exp\left[(\alpha_a-\alpha_s)\,l\right]. \tag{3}$$

From the Eq. (3), it can be seen that Raman scattering signal is not only modulated by the environmental temperature, but also associated with some inherent parameters of the fiber (K_s, υ_s and α_a, *et al.*). Traditional pre-calibration stage requires the entire fiber to a constant temperature condition for calibrating this inherent parameter. To omit this pre-calibration process, a section of reference fiber be set at the front of sensing fiber to calibrate the temperature measurement result. The backward scattering intensity ratio of Stokes over anti-Stokes signal at the reference fiber can be expressed as:

$$\frac{\phi_{sb}^{re}}{\phi_{ab}^{re}} = \frac{K_s}{K_a}\left(\frac{\upsilon_s}{\upsilon_a}\right)^4 \exp\left(-\frac{h\Delta v}{kT_r}\right)\exp\left[(\alpha_a-\alpha_s)\,L_r\right]. \tag{4}$$

Where the ϕ_{sb}^{re} and ϕ_{ab}^{re} are the backward scattering intensity of Stokes and anti-Stokes at the reference fiber respectively, T_r and L_r are the temperature and position of reference fiber. In addition, the forward scattering intensity ratio of Stokes over anti-Stokes signal at the reference fiber can be expressed as:

$$\frac{\phi_{sf}^{re}}{\phi_{af}^{re}} = \frac{K_s}{K_a}\left(\frac{\upsilon_s}{\upsilon_a}\right)^4 \exp\left(-\frac{h\Delta v}{kT_r}\right)\exp\left[(\alpha_a-\alpha_s)\,(l-L_r)\right]. \tag{5}$$

Where the ϕ_{sf}^{re} and ϕ_{af}^{re} are the forward scattering intensity of Stokes and anti-Stokes at the reference fiber respectively. The Raman intensity in the loop configuration can be obtained by

$$\sqrt{\frac{\phi_{sb}^{re}}{\phi_{ab}^{re}}\frac{\phi_{sf}^{re}}{\phi_{af}^{re}}} = \frac{K_s}{K_a}\left(\frac{\upsilon_s}{\upsilon_a}\right)^4 \exp\left(-\frac{h\Delta v}{kT_r}\right)\exp\left[(\alpha_a-\alpha_s)\,l\right]. \tag{6}$$

Using the Eqs. (3) and (6), we can get the temperature demodulation results from Eq. (7). And it can be seen from that the Raman signal is only modulated by temperature. Moreover, this temperature demodulation method not only has the advantage of loop configuration (eliminate the influence of external physical perturbation on the temperature measurement results [32]), but it can also omit the pre-calibration process before measurement.

$$\frac{1}{T} = \left[\ln\left(\frac{\sqrt{\phi_{sb}\phi_{sf}/\phi_{ab}\phi_{af}}}{\sqrt{\phi_{sb}^{re}\phi_{sf}^{re}/\phi_{ab}^{re}\phi_{af}^{re}}}\right)\cdot\left(-\frac{k}{h\Delta v}\right)\right] + \frac{1}{T_r}. \tag{7}$$

2.2 Fiber Loss Based on OTDR Technology for Crack Measurement

The information of structure's crack is extracted by using the loss characteristics of Raman Stokes, which is based on OTDR technology. Compared to the Raman anti-Stokes signal, the Raman Stokes intensity is higher, and not sensitive to temperature [10]. The fiber loss schematic based on OTDR for crack measurement is shown in Fig. 2. When the tension (caused by structural cracks) is applied to the sensing fiber, it will produce a deformation at this point. And this deformation affects the effective scattering area and luminous flux in the sensing fiber, which ultimately leads to a larger loss at this point. In addition, the different degrees of tension are applied in the sensing fiber, the loss characteristics will appear in different states. Specifically, the fiber loss will increase as the tension rises. The specific method is as follows:

Before the measurement, the system needs to obtain the Stokes scattering intensity when the sensing fiber maintains a relaxed state. In this state, the Raman intensity of Stokes based on OTDR

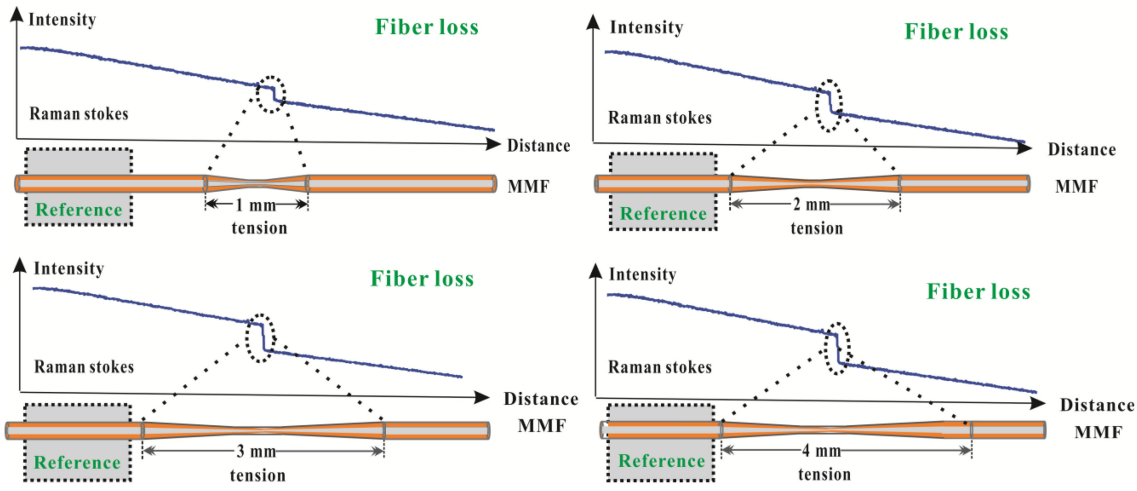

Fig. 2. Crack measurement schematic based on fiber loss.

technology can be expressed as:

$$\phi_{sc} = K_s \upsilon_s^4 \frac{1}{1+\exp\left[\left(h\Delta v/kT_c\right)-1\right]}\left[\left(\alpha_o+\alpha_s\right)L\right] \tag{8}$$

In addition, the ratio of Stokes intensity at the entire sensing (ϕ_{sc}) over the Stokes intensity at the reference fiber (ϕ_{sc}^{re}) can be expressed as:

$$\frac{\phi_{sc}}{\phi_{sc}^{re}} = \frac{1+\exp\left[\left(h\Delta v/kT_c^r\right)-1\right]}{1+\exp\left[\left(h\Delta v/kT_c\right)-1\right]} \times \left[\left(\alpha_o+\alpha_s\right)\left(L-L_r\right)\right]. \tag{9}$$

Where T_c and T_c^r stand for the temperature of sensing fiber and reference fiber, L_r stands for the position of the reference fiber.

In the measurement stage, the fiber tension induced by structure crack will influence the fiber loss, which leads to the Stokes intensity that modulated by the structure tension. In this letter, *S(L)* is defined as the tension modulation factor on the Stokes signal. The ratio of Stokes intensity at the entire sensing (ϕ_s) over the Stokes intensity at the reference fiber (ϕ_{sr}) can be expressed as:

$$\frac{\phi_s}{\phi_s^{re}} = S(L) \times \frac{1+\exp\left[\left(h\Delta v/kT^r\right)-1\right]}{1+\exp\left[\left(h\Delta v/kT\right)-1\right]} \times \left[\left(\alpha_o+\alpha_s\right)\left(L-L_r\right)\right]. \tag{10}$$

Where T^r stands for the temperature at the reference fiber. Then the crack information can be derived using the Eqs. (9) and (10). The demodulation equation of crack information can be expressed as:

$$S(L) = \frac{\phi_{sc}^{re}}{\phi_{sc}}\frac{\phi_s}{\phi_s^{re}} \times \frac{1+\exp\left[\left(h\Delta v/kT\right)-1\right]}{1+\exp\left[\left(h\Delta v/kT^r\right)-1\right]} \frac{1+\exp\left[\left(h\Delta v/kT_c^r\right)-1\right]}{1+\exp\left[\left(h\Delta v/kT_c\right)-1\right]}. \tag{11}$$

We can use the Eq. (11) to demodulate the crack information, it can be observed that the temperature information along the sensing fiber should firstly be detected, before the crack information is extracted.

3. Experimental Setup

The experimental setup of temperature and crack measurement is shown in Fig. 3. The R-DTS consists of a pulse modulator, wavelength division multiplexer (WDM), Analog-to-Digital Converter (ADC), optical switch, two avalanche photodiodes (APD) and amplifier receivers. The APD and

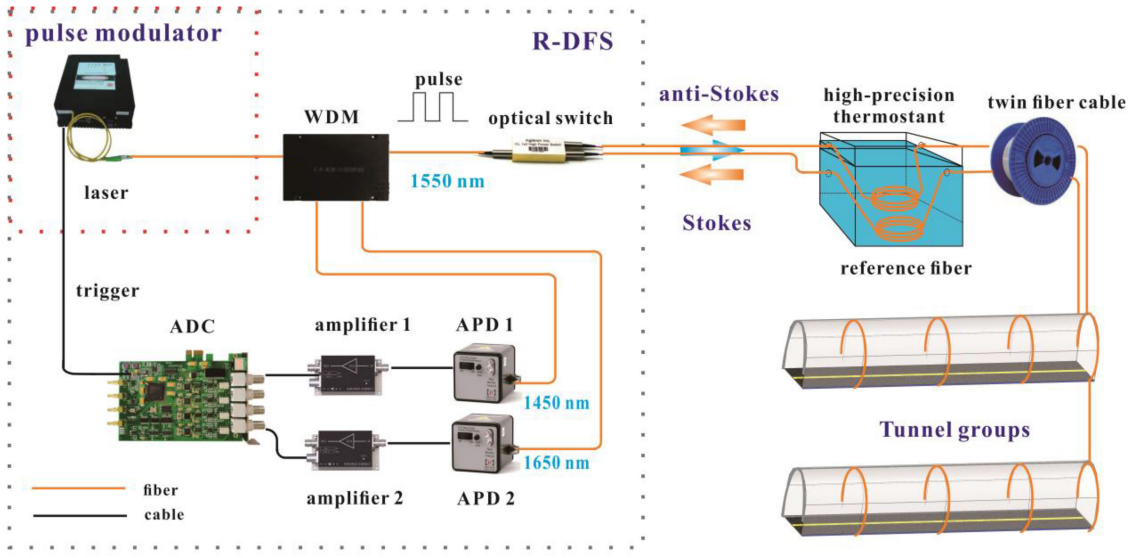

Fig. 3. Experimental setup. WDM: wavelength division multiplexer; APD: avalanche photodiode; Amp: amplifier; ADC: Analog-to-Digital Converter.

TABLE 1
Key Device Parameters of the R-DTS

Device	Manufacturer	Parameters
Pulse modulator	CONNET LASER	Wavelength: 1550 nm
WDM	XUFENG PHOTOELECTRIC	1450, 1550, 1650 nm
APD	FBY PHOTOELECTRIC	Bandwidth:100 MHz
Amplifier	REBES	Bandwidth:100 MHz
ADC	JEMETECH	4 channels
Sensing fiber	YOFC	Multimode, 62.5/125 um
High-precision thermostat	NANJING KENFAN ELECTRONIC	Temperature fluctuation: 0.05 °C

DAC are demodulation devices for collecting and demodulating the data. The pulsed laser source operates at about 1550 nm wavelength with a pulse width of 10 ns and a repetition rate of 5 kHz. The pulses with 15 W are launched into the sensing fiber (graded-index multimode, 62.5/125, MMF). The WDM is used to control the back-scattering light. The function of the WDM is to filter the Stokes light (1650 nm) and the anti-Stokes light (1450 nm) from the back-scattering light coming to towards the laser source. The isolation degree ranges from 35 dB to 40 dB for the anti-stokes part. Then the Stokes and anti-Stokes light is then detected simultaneously by two low-noise APDs through WDM. Then the electrical signals are collected by an ADC. Finally, they are transmitted to a computer for further data processing. The function of the optical switch is changing the incident light enters the direction of the sensing fiber, for collecting Raman scattering light of forward and backward direction. The reference fiber is placed in a high-precision thermostat to control the temperature of the reference fiber (T_r). Compared to the traditional combined sensors, the proposed system is simple and suitable for industrial application. The key device parameters of the R-DTS are shown in Table 1.

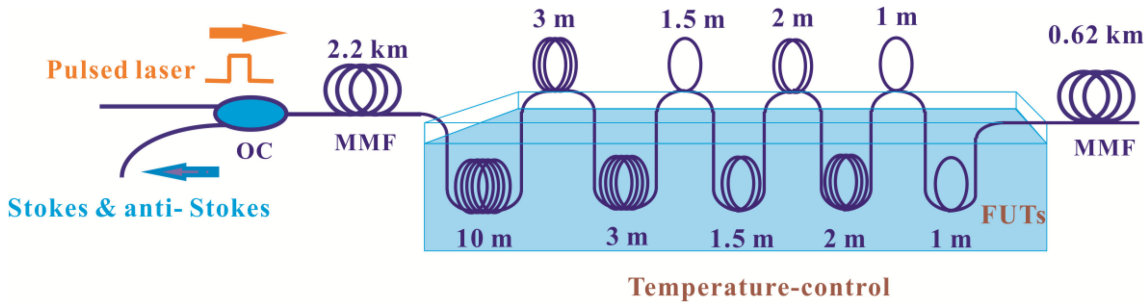

Fig. 4. Sensing fiber distribution in the temperature experiment.

We can use the same technique with single mode fibers to detect temperature along the sensing fiber and structural crack. However, the fiber devices (including laser, WDM, optical switch, MMF) in the system are all using the single mode fiber before measurement. In addition, the proposed R-DTS system does not operate at any given wavelength, it is only suitable for laser system with 1550 nm.

4. Results and Analysis

4.1 Temperature Measurement

In the temperature measurement experiment, distributed temperature measurement is carried out by using the graded-index multimode sensing fiber (twin-fiber cable, 62.5/125 um, twin-fiber cable for simultaneously collecting backward and forward direction Raman signal). The sensing fiber configuration is shown in Fig. 4. To detect the temperature along the sensing fiber, the multimode fiber with 3 km range has been used. (The fiber length of the single core is 3 km, and the total length of the two-fiber cable is 6 km. Fig. 4 shows the fiber length of the single core.) Among them, the fiber under test (FUT) consists of five sections with a length of 10 m, 3 m, 1.5 m, 2 m and 1 m. The temperature of FUT is set at 35 °C, 40 °C, 45 °C, 50 °C, 55 °C, 60 °C and 65 °C by the temperature-control chamber (TCC) and the rest of the sensing fiber is maintained at room temperature (the room temperature is about 23 °C). The temperature measurement result of overall distribution based on the Eq. (7) are obtained in Fig. 5. The Fig. 5(a)–(g) stands for the overall distribution of the temperature measurement results (The results are averaged 1 k times and denoised by wavelet transform modulus maximum. This denoise method is available to capture singular points of signal when the signal has a low signal to noise ratio [12]). Fig. 5(h) stands for the temperature results of FUTs under the control of the TCC. It can be observed that the temperature demodulation method proposed in this letter can distinguish between the temperature of TCC and room temperature, and the R-DTS can accurately measure the temperature distribution along the FUT. In addition, this temperature demodulation method can not only eliminate the influence of external physical perturbation on the temperature measurement results (the advantage of loop configuration [32]), but also does not require any pre-calibration process before measurement.

Then we analyze the temperature measurement accuracy and spatial resolution of the R-DTS. The temperature measurement accuracy represents the difference between the values of actual measured temperature and the standard temperature. And the temperature measurement accuracy and error bar are shown in Fig. 6. It can be observed that the temperature measurement accuracy is 0.28 °C at the sensing distance of 2.3 km by measuring the average of the all data. The limitation of temperature measurement accuracy is the signal-to-noise ratio of R-DTS system. The spatial resolution indicates that the R-DTS system can resolve the minimum spatial distance of temperature change, which reflects the sensitivity of the system to position perception, that is an important performance indicator of R-DTS. The result of the spatial resolution is shown in Fig. 6(b) (10%–90% response distance to a temperature step). Fig. 6(b) shows the spatial resolution of the FUT under the temperature-control chamber of 65 °C, and the relevant spatial resolution is 1.2 m.

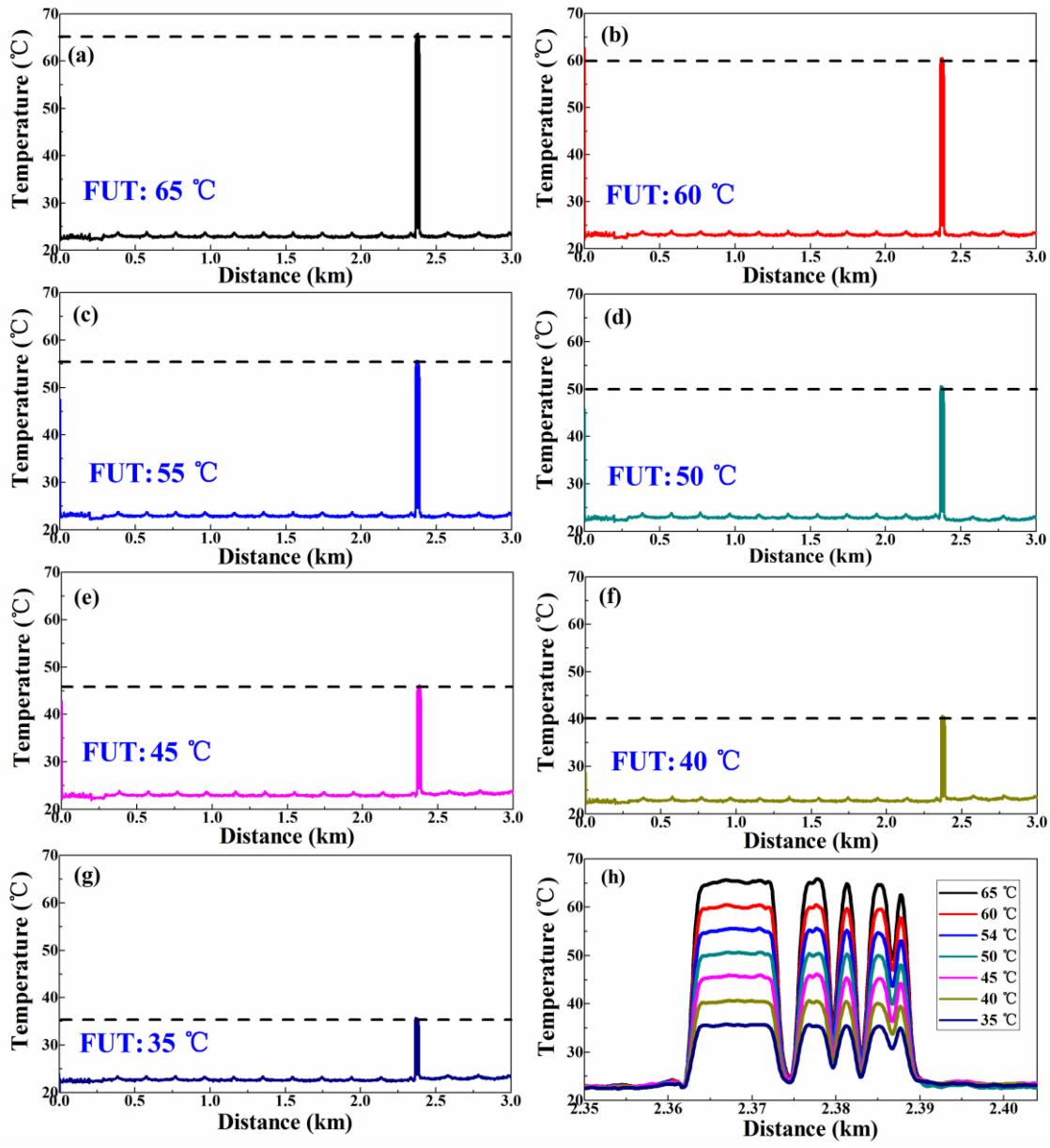

Fig. 5. The overall-distribution of the temperature measurement results under the control of the (a) 65 °C, (b) 60 °C, (c) 55 °C, (d) 50 °C, (e) 45 °C, (f) 40 °C and (g) 35 °C. (h) The results of temperature distribution of FUTs.

The limitation of spatial resolution is the pulse width of laser due to the principle of OTDR. In this experiment, the pulse width of the laser is 10 ns, and the theoretical spatial resolution is 1 m. However, due to the influence of fiber dispersion, the actual spatial resolution of the system is 1.2 m. In addition, the temperature performance parameters of R-DTS are shown in Table 2.

4.2 Structure's Crack Measurement

In the experiment of crack measurement, the sensing fiber distribution is shown in Fig. 7. We use the crack simulator (HWHR Instruments, A052F) to apply axial tension on the multimode sensing fiber for simulating the generation of structure crack. (The displacement of HWHR Instruments can

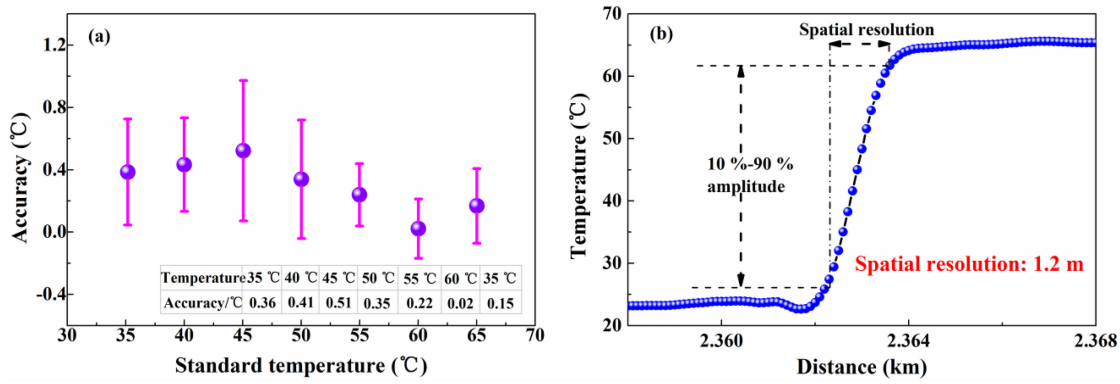

Fig. 6. (a) Temperature accuracy and (b) spatial resolution at the sensing distance of 2.3 km.

TABLE 2
Performance Parameters of R-DTS

Parameters	Values
Temperature accuracy	0.28 °C
Temperature resolution	0.57 °C
Sensing distance	2.4 km
Response time	1.04 s
Spatial resolution	1.2 m

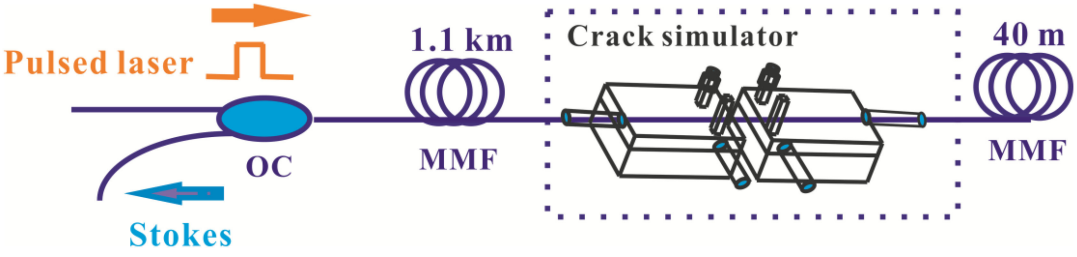

Fig. 7. Sensing fiber distribution in the crack measurement experiment.

be manually adjusted to extension the fiber.) The graded-index multimode sensing fiber with 1.1 km range which is connected to the optical circulator (OC) at one end, and the other end is connected to the crack simulator. The 40 m sensing fiber is attached to the other end of the fiber stretcher.

During the experimental stage, we apply the varying degree of axial tension to the multimode sensing fiber at 1.1 km, then the Raman Stokes signal is collected by the DAC. After demodulated by the Eq. (11), the distribution information of fiber loss is obtained, as shown in Fig. 8(a)–(h). Fig. 8(i) represents the loss variation of Stokes at the position of 1.1 km, which under the different degrees of axis tension (crack). From the experimental results, it can be seen that the fiber loss changes greatly at 1.1 km where the structure crack is generated. The fiber loss presents different status under the varying degree of axial tension. Specifically, the fiber loss increases when the crack rising. The experimental results are identical with the theoretical analysis. In addition, Fig. 9 stands for the relationship between fiber loss coefficient and crack information, which shows the fiber loss coefficient keeps a good linear variation between the ranges of 1.6 mm and 5.6 mm. And the fitting degree of coefficient can reach up to 0.98801. It represents that the crack information can be obtained by using the fiber loss of Raman Stokes. And the measurement range from 1.6 mm

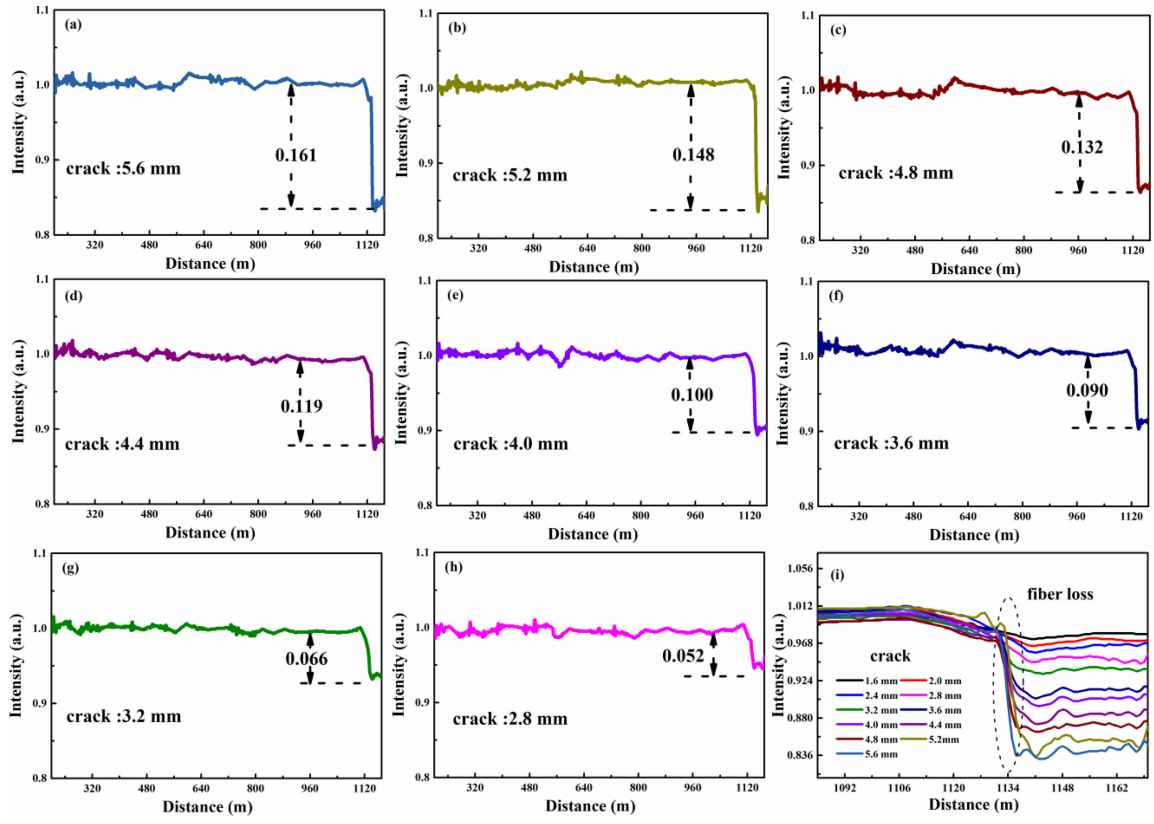

Fig. 8. (a–h) The overall-distribution of fiber loss measurement results under the different crack. (i) The fiber loss distribution results of FUTs.

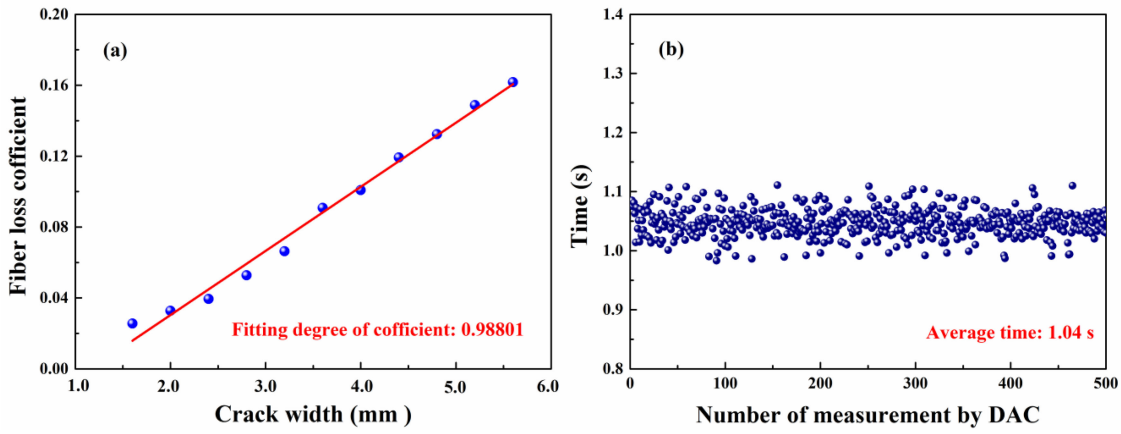

Fig. 9. (a) The relationship between fiber loss coefficient and crack information. (b) The measurement time of system.

to 5.6 mm is suitable for large-scale crack monitoring of structures. In addition, the fundamental limitation of cracking resolution measurement is the signal-to-noise ratio of R-DTS system. The experiment result shows the resolution of crack is 0.4 mm. If the system's signal-to-noise ratio is increased, the cracking resolution will also be optimized. Moreover, the measurement time of this method is only related to the acquisition time of DAC, as shown in Fig. 9(b), the average measurement time can reach up to 1.04 s.

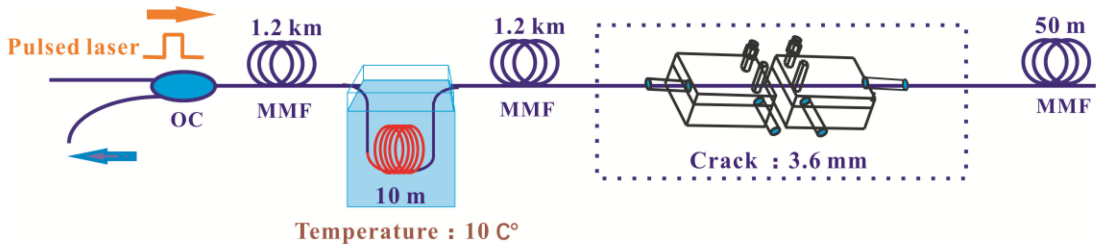

Fig. 10. The sensing fiber distribution in the experiment.

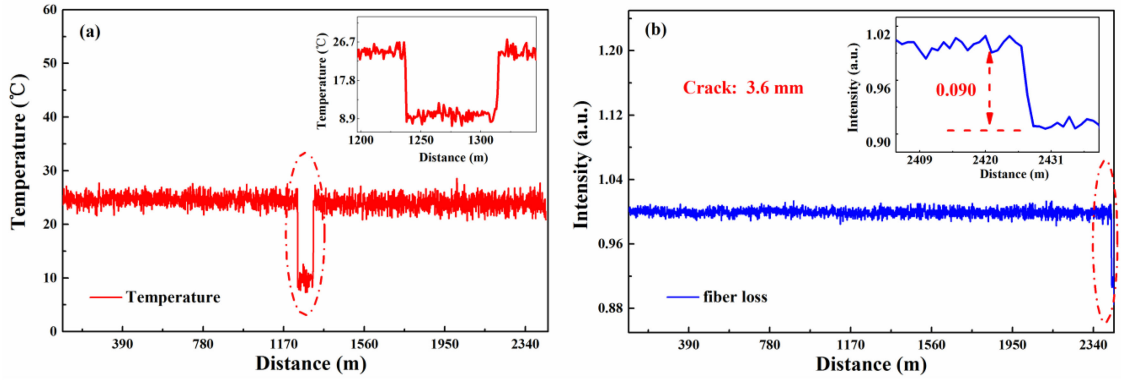

Fig. 11. (a) Temperature and (b) crack measurement results using one sensing fiber.

4.3 Simultaneous Temperature and Crack Measurement

In order to prove that this method (based on Eqs. 7 and 11) can achieve the temperature and crack measurement using one fiber, we apply the temperature and axial extension on the sensing fiber at the same time. The distribution of sensing fiber is shown in Fig. 10, we place a fiber under test 1 (FUT 1, 60 m) at the position of the 1.2 km and set the temperature to 10 °C. The fiber under test 2 (FUT 2, 1 m) is placed at the position of 2.4 km, and is stretched to produce the axial tension using the crack simulator (the crack is 3.6 mm).

The distribution results of temperature and fiber loss are shown in Fig. 11. The demodulation signals are all averaged 10 k times, and it has not undergone any denoising method. The Fig. 11(a) stands for the temperature distribution results along the sensing fiber, that clearly distinguishes the temperature distribution of FUT 1 (10 °C) and the environment temperature (23 °C). Fig. 11(b) represents the distribution results of fiber loss. And we can see from the illustration of Fig. 11(b) that the fiber loss coefficient at 2.4 km is 0.090. According to the relationship between the fiber loss and the crack in Fig. 9(a), it can be observed that the detected crack at 2.4 km is 3.6 mm. The experimental results show that the crack monitored by the fiber loss is consistent with the parameters set by crack simulator. This experiment illustrates that the proposed optic-fiber sensor can detect the temperature and large-scale crack using one sensing fiber.

5. Discussion and Conclusion

The performance improvement of temperature accuracy and cracking measurement accuracy depend on the signal-to-noise ratio of R-DTS system. In the experiment, the denoising method of cumulative average and wavelet transform modulus maximum are applied to the Raman signal. In order to further improve the R-DTS system performance, we will optimize the system's signal-to-noise ratio (such as eliminate the environmental noise) in the next step.

In summary, we propose and experimentally demonstrate a novel optic-fiber sensor and demodulation method to measure the temperature and structure's crack. The proposed method is based on the Raman loop configuration with reference fiber to extract temperature along the sensing fiber, which can not only eliminate the influence of external physical perturbation on temperature measurement results, but also does not require pre-calibration process before measurement. The experimental results show that the temperature accuracy and spatial resolution can reach up to 0.28 °C and 1.2 m under the response time of 1.04 s. This proposed method improves the engineering applicability of optic-fiber sensors. In addition, the information of crack is detected by using the fiber loss characteristics based on OTDR technology. The experimental results show that the fiber loss coefficient keeps a good linear variation between the crack ranges of 1.6 mm and 5.6 mm, and the fitting degree of coefficient can reach up to 0.98801. The experiment also proves that the temperature and crack can be measured by using only one sensing fiber.

References

[1] M. J. Zhang *et al.*, "Impact of Brillouin amplification on the spatial resolution of noise-correlated Brillouin optical reflectometry," *Chin. Opt. Lett.*, vol. 15, no. 8, 2017, Art. no. 080603.

[2] X. H. Fu, H. Y. Xie, C. Q. Yang, S. Y. Zhang, G. W. Fu, and W. H. Bi, "Research on the temperature sensing characteristics of triple cladding quartz specialty fiber based on cladding mode resonance," *Acta. Phys. Sinica* vol. 65, no. 2, pp. 167–175, 2016.

[3] G. Tu, X. Zhang, Y. Zhang, F. Zhu, L. Xia, and B. Nakarmi, "The development of an-OTDR system for quantitative vibration measurement," *IEEE Photon. Technol. Lett.*, vol. 27, no. 12, pp. 1349–1352, Jun. 2015.

[4] D. Jong, J. D. Slingerland, and V. D. Van, "Fiber optic distributed temperature sensing for the determination of air temperature," *Atmos. Meas. Tech.*, vol. 8, no. 1, pp. 335–339, 2014.

[5] D. Hwang, D. J. Yoon, I. B. Kwon, D. C. Seo, and Y. Chung, "Novel auto-correctin method in a fiber-optic distributed-temperature sensor using reflected anti-Stokes Raman scattering," *Opt. Exp.*, vol. 18, no. 10, pp. 9747–9754, 2010.

[6] Z. N. Wang, Y. J. Rao, and H. Wu, "Long-distance fiber-optic point-sensing systems based on random fiber lasers," *Opt. Exp.*, vol. 20, no. 16, pp. 17695–17700, 2012.

[7] J. D. Zhang, T. Zhu, H. Zhou, S. H. Huang, M. Liu, and W. Huang, "High spatial resolution distributed fiber system for multi-parameter sensing based on modulated pulses," *Opt. Exp.*, vol. 24, no. 24, pp. 27482–27493, 2016.

[8] Y. G. Lu, Z. G. Qin, P. Lu, D. P. Zhou, L. Chen, and X. Y. Bao, "Distributed strain and temperature measurement by Brillouin beat spectrum," *IEEE Photon. Technol. Lett.*, vol. 25, no. 11, pp. 1050–1053, Jun. 2013.

[9] S. M. Maughan, H. H. Kee, and T. P. Newson, "Simultaneous distributed fibre temperature and strain sensor using microwave coherent detection of spontaneous Brillouin backscatter," *Meas. Sci. Technol.*, vol. 12, no. 7, pp. 834–842, 2001.

[10] J. Li, B. Q. Yan, M. J. Zhang, J. Z. Zhang, L. J. Qiao, and T. Wang, "Auto-correction method for improving temperature stability in a long-range Raman fiber temperature sensor," *Appl. Opt.*, vol. 58, no. 1, pp. 37–42, 2019.

[11] M. Wang *et al.*, "Few-mode fiber based Raman distributed temperature sensing," *Opt. Exp.*, vol. 25, no. 5, pp. 4907–4916, 2017.

[12] J. Li *et al.*, "Performance improvement of Raman distributed temperature system by using noise suppression," *Photon. Sensors*, vol. 28, no. 2, pp. 103–113, 2017.

[13] B. Huang and X. Shu, "Ultra-compact strain- and temperature-insensitive torsion sensor based on a line-by-line inscribed phase-shifted FBG," *Opt. Exp.*, vol. 24, no. 16, pp. 17670–17679, 2016.

[14] N. Kuse, A. Ozawa, and Y. Kobayashi, "Static FBG strain sensor with high resolution and large dynamic range by dual-comb spectroscopy," *Opt. Exp.*, vol. 21, no. 9, pp. 11141–11149, 2013.

[15] B. Hopf, A. W. Koch, and J. Roths, "Temperature dependence of glue-induced birefringence in surface-attached FBG strain sensors," *J. Lightw. Technol.*, vol. 34, no. 4, pp. 1220–1227, Feb. 2016.

[16] Q. Bai *et al.*, "A Logarithmic detection scheme in BOTDR With low-bandwidth requests," *IEEE Access*, vol. 6, pp. 74828–74835, 2018.

[17] M. A. Soto, J. A. Ramírez, and L. Thévenaz, "Intensifying the response of distributed optical fibre sensors using 2D and 3D image restoration," *Nat. Commun.*, vol. 7, no. 10870, pp. 1–11, 2016.

[18] Y. Mizuno, "Proposal of Brillouin optical correlation-domain reflectometry (BOCDR)," *Opt. Exp.*, vol. 16, no. 16, pp. 12148–12153, 2008.

[19] J. Z. Zhang *et al.*, "Chaotic Brillouin optical correlation domain analysis," *Opt. Lett.*, vol. 43, no. 8, pp. 1722–1725, 2018.

[20] C. S. Kim, T. H. Lee, Y. S. Yu, Y. G. Han, and M. Y. Jeong, "Multi-point interrogation of FBG sensors using cascaded flexible wavelength-division Sagnac loop filters," *Opt. Exp.*, vol. 14, no. 19, pp. 8546–51, 2006.

[21] R. J. Williams *et al.*, "Point-by-point inscription of apodized fiber Bragg gratings," *Opt. Lett.*, vol. 36, no. 15, pp. 2988–2990, 2011.

[22] Y. G. Lu, Z. G. Qin, P. Lu, D. P. Zhou, L. Chen, and X. Y. Bao, "Distributed strain and temperature measurement by Brillouin beat spectrum," *IEEE Photon. Technol. Lett.*, vol. 25, no. 11, pp. 1050–1053, Jun. 2013.

[23] Y. K. Dong, L. Chen, and X. Y. Bao, "High-spatial-resolution time-domain simultaneous strain and temperature sensor using Brillouin scattering and Birefringence in a polarization-maintaining fiber," *IEEE Photon. Technol. Lett.*, vol. 22, no. 18, pp. 1364–1366, Sep. 2010.

[24] G. Bolognini and M. A. Soto, "Optical pulse coding in hybrid distributed sensing based on Raman and Brillouin scattering employing Fabry-Perot lasers," *Opt. Exp.*, vol. 18, no. 8, pp. 8459–8465, 2010.
[25] S. M. Maughan, H. H. Kee, and T. P. Newson, "Simultaneous distributed fibre temperature and strain sensor using microwave coherent detection of spontaneous Brillouin backscatter," *Meas. Sci. Technol.*, vol. 12, no. 7, pp. 834–842, 2001.
[26] W. W. Zou, Z. Y. He, and K. Hotate, "Complete discrimination of strain and temperature using Brillouin frequency shift and birefringence in a polarization-maintaining fiber," *Opt. Exp.*, vol. 17, no. 3, pp. 1248–1255, 2009.
[27] B. N. Sun *et al.*, "Accuracy improvement of Raman distributed temperature sensors based on eliminating Rayleigh noise impact," *Opt. Commun.*, vol. 306, pp. 117–120, 2013.
[28] D. Hwang, D. J. Yoon, I. B. Kwon, D. C. Seo, and Y. Chung, "Novel auto-correction method in a fiber-optic distributed-temperature sensor using reflected anti-Stokes Raman scattering," *Opt. Exp.*, vol. 18, no. 10, pp. 9747–9754, 2010.
[29] J. Park *et al.*, "Raman-based distributed temperature sensor with simplex coding and link optimization," *IEEE Photon. Technol. Lett.*, vol. 18, no. 17, pp. 1879–1881, Sep. 2006.
[30] J. Li *et al.*, "Long-range raman distributed fiber temperature sensor with early warning model for fire detection and prevention," *IEEE Sensors J .*, vol. 19, no. 10, pp. 3711–3717, May 2019.
[31] M. A. Soto, "Raman-based distributed temperature sensor with 1 m spatial resolution over 26 km SMF using low-repetition-rate cyclic pulse coding," *Opt. Lett.*, vol. 36, no. 13, pp. 2557–2559, 2011.
[32] M. A. Soto, A. Signorini, T. Nannipieri, S. Faralli, and G. Bolognini, "High-performance raman-based distributed fiber-optic sensing under a loop scheme using anti-stokes light only," *IEEE Photon. Technol. Lett.*, vol. 23, no. 9, pp. 534–536, May 2011.